Am J Physiol Cell Physiol 331: C864–C876, 2026.
First published August 11, 2026; doi:10.1152/ajpcell.00055.2026

american physiological society

AMERICAN JOURNAL OF PHYSIOLOGY
CELL PHYSIOLOGY

RESEARCH ARTICLE

Human M1 macrophages secrete glutamine: a role for the transporters ASCT2 and SNAT5

Giuseppe Taurino,[1] Martina Chiu,[1] Chiara Ughini,[1] Chiara Maccari,[2,3] Roberta Andreoli,[2,3] Giulia Longhi,[4,5] Marco Ventura,[4,5] Ovidio Bussolati,[1,5] and Massimiliano G. Bianchi[1,5]

[1]*Laboratory of General Pathology, Department of Medicine and Surgery, University of Parma, Parma, Italy;* [2]*Laboratory of Industrial Toxicology, Department of Medicine and Surgery, University of Parma, Parma, Italy;* [3]*Center of Excellence for Toxicological Research (CERT), University of Parma, Parma, Italy;* [4]*Laboratory of Probiogenomics, Department of Chemistry, Life Sciences and Environmental Sustainability, University of Parma, Parma, Italy; and* [5]*Microbiome Research Hub, University of Parma, Parma, Italy*

Abstract

Previous results indicated that LPS treatment of human macrophages is associated with the induction of glutamate-ammonia-ligase (GLUL), the enzyme that synthesizes glutamine (Gln), although the effects on cell Gln level were not assessed by those studies. Here, we show that M1 polarization of human THP-1 macrophage-like cells with LPS and interferon γ (IFNγ) induces not only GLUL but also the exchange Gln transporter ASCT2 and the bidirectional carrier SNAT5. Consequently, Gln influx markedly increases, with ASCT2 and SNAT5 inhibitors suppressing the effect. Notwithstanding these changes, cell Gln is comparable in human M0 and M1 macrophages. However, under Gln-free conditions, Gln efflux is threefold faster in M1 macrophages. With the same approach, we have demonstrated that cell glutamate (Glu) mostly derives from extracellular Gln. Furthermore, Glu efflux is markedly higher in M1 macrophages, consistent with the induction of the Glu-cystine exchanger xCT. Induction of GLUL, SNAT5, and xCT, along with SNAT5-dependent stimulation of Gln transport, are clearly detectable also in primary human macrophages, derived from monocytes of peripheral blood and M1-polarized with LPS/IFNγ. These data indicate that, through a stimulation of Gln and Glu efflux, M1-polarized human macrophages can increase the concentration of both amino acids in the extracellular microenvironment.

NEW & NOTEWORTHY M1 polarization of human macrophages promotes the induction of glutamate-ammonia-ligase (GLUL) and of the Gln transporters SNAT5 and ASCT2, leading to a faster efflux of the amino acid into the extracellular compartment. Under the same conditions, induction of the transporter xCT mediates the increased efflux of glutamate. Therefore, M1 macrophages can increase the extracellular concentrations of both glutamine and glutamate, potentially influencing the metabolic and functional behavior of other cell populations present in the microenvironment.

GLUL; glutamate; glutamine synthetase; LPS; SLC38A5

INTRODUCTION

Activation and polarization of human macrophages are associated with specific metabolic changes, with M1-like macrophages displaying enhanced glycolysis, whereas, in contrast, M2-like cells are more oxidative (1).

Glutamine (Gln) metabolism is also affected, with consumption of the amino acid increasing during M1 activation (2). In macrophages infected with *Mycobacterium tuberculosis*, Gln serves as a carbon and nitrogen source for metabolic reprogramming and the synthesis of succinate, aspartate, and itaconate (3). However, Gln plays a variety of metabolic roles, and, therefore, the functional significance of these changes in macrophage biology is not yet fully understood.

Previous results (4, 5) have demonstrated that long-term exposure of human macrophages to LPS causes an increase in the expression of glutamate-ammonia-ligase (GLUL), the enzyme that obtain Gln from glutamate (Glu) and ammonium. This change requires at least 24 h of exposure to endotoxin and is attributable to the induction of *GLUL*. GLUL expression and activity relate to metabolic changes occurring during macrophage activation and polarization, with GLUL inhibition driving cells toward M1 polarization (6).

GLUL activity is a determinant for the intracellular level of Gln, and its shelf-life is inversely regulated at the protein level by the amino acid availability (7). However, cell Gln content is determined not only by the enzymes that synthesize or consume the amino acid but also by its membrane transport and, therefore, by its extracellular concentration. In human cells, transmembrane Gln fluxes are mediated by several carriers, which operate exchange or unidirectional fluxes (8–10). Among these, system A transporters of the

Correspondence: M. G. Bianchi (massimiliano.bianchi@unipr.it).
Submitted 23 January 2026 / Revised 2 August 2026 / Accepted 3 August 2026

0363-6143/26 Copyright © 2026 The Authors. Licensed under Creative Commons Attribution CC-BY-NC-ND 4.0.
Published by the American Physiological Society.

Downloaded from journals.physiology.org/journal/ajpcell at Univ Degli Studi Di Parma Biblio Centrale (160.078.086.043) on September 21, 2026.

SLC38 family, such as SNAT1 and SNAT2 (coded by *SLC38A1* and *SLC38A2*, respectively), are unidirectional, secondary active, sodium-dependent carriers (11). ASCT2, coded by *SLC1A5*, is a sodium-dependent exchanger (12). SNAT3 and SNAT5, coded by *SLC38A3* and *SLC38A5*, respectively, are system N carriers, which can mediate both net efflux and influx of their substrates depending on their transmembrane gradients (13). Notably, *SLC38A5*/SNAT5 has been found to be involved in several metabolic cross talks involving intercellular Gln and asparagine fluxes (14, 15). Alkaline medium pH stimulates both SNAT2 and SNAT5 (11, 16).

To achieve a better understanding of changes in Gln metabolism and transport associated with macrophage activation and polarization, we have polarized two human macrophage models: the monocytic cell line THP-1 and primary macrophages from peripheral blood monocytes (MDMs), under a typical M1-promoting condition, consisting of the combined treatment with LPS and interferon γ (IFNγ). Along with GLUL induction, the incubation of human macrophages with LPS and IFNγ elicits expression changes of several Gln transporters, leading to an increase in Gln membrane transport that is sensitive to SNAT5 inhibitors. Overall, these changes do not appear to significantly modify cell Gln content but, rather, the efflux of Gln and Glu into the extracellular compartment.

MATERIALS AND METHODS

Cells and Treatments

Acute monocytic leukemia THP-1 cells (male, 1 yr), obtained from the Cell Bank of the Istituto Zooprofilattico Sperimentale della Lombardia ed Emilia-Romagna (Brescia, Italy), were cultured in RPMI 1640 (Euroclone, Milan, Italy) supplemented with 2 mM Gln (Sigma-Aldrich), antibiotics (100 U/mL penicillin and 100 μg/mL streptomycin), and 10% fetal bovine serum (Gibco, Thermo Fisher Scientific, Milan, Italy). Macrophage-like differentiation was obtained by incubating THP-1 cells in phorbol myristate acetate (80 nM) for 3 h. After three washes in phosphate-buffered saline (PBS), cells were rescued in fresh medium for 24 h before treatment. For the experiments, Gln concentration was kept at 0.6 mM, in the physiological range of human plasma Gln. Macrophage stimulation was performed by adding LPS (*Escherichia coli* strain O55:B5; Sigma-Aldrich, 100 ng/mL) and interferon γ (IFNγ; R&D Systems, Bio-Techne, Milan, Italy, 20 ng/mL) to the culture medium for the periods specified in each experiment.

The protocol for isolation and use of primary human macrophages was reviewed and approved by the Ethical Committee AVEN (325/2024/TESS/UNIPR). Written informed consent was obtained from all the donors. Peripheral blood mononuclear cells (PBMCs) were isolated from peripheral blood aliquots obtained from healthy subjects. Aliquots of 30 mL of blood were diluted 1:3 in PBS, and equal volumes of the solution (22 mL) were carefully dispensed on 15 mL of Ficoll-Paque Plus (GE Healthcare Life Sciences, Pittsburgh, PA) in four sterile conical tubes. After 30 min of centrifugation at 400 *g* in a swinging-bucket rotor without brake, buffy coat fractions of PBMC were harvested and pulled into a new tube. Cells were then suspended, centrifuged at 200 *g* for 10 min, and repeatedly washed with 50 mL of PBS to remove red blood cells and platelet contamination. Purified PBMCs were resuspended in RPMI 1640 culture medium supplemented with 5% of A/B human serum at a density of 3×10^5 cells/mL and seeded in either a 24-well culture plate (1 mL/well) to perform RT-PCR experiments, Western blot, and amino acid determination or a 96-well culture dish (200 μL/well) for influx experiments. After 30 min of incubation in standard culture conditions (37°C at 5% CO_2), adherent monocytes were rinsed three times with PBS to remove residual lymphocytes and platelets. Culture medium was then renewed, and cells were incubated for 7 days in the presence of macrophage-colony stimulating factor (M-CSF) (R&D Systems, 50 ng/mL) to achieve differentiation into monocyte-derived macrophages (MDM). For M1 polarization, MDM were stimulated with LPS (5 ng/mL) and IFNγ (20 ng/mL).

Gene Expression

The extraction of total RNA was performed using the GeneJET RNA Purification Kit (Life Technologies, Thermo Fisher Scientific, Milan, Italy), following the manufacturer's instructions. In brief, 250 ng of total RNA were reverse-transcribed, and aliquots of 12 ng of cDNA were amplified in a total volume of 10 μL with PowerUp SYBR Green Master mix (Thermo Fisher Scientific, Milan, Italy), along with the forward and reverse primers (5 pmol each), reported in Table 1. Real-time PCR (RT-PCR) was performed in a QuantStudio 3 apparatus (Life Technologies, Thermo Fisher Scientific), setting a denaturation step at 95°C for 15 s, which was followed by the annealing (15 s) and extension (1 min) steps at a temperature characteristic for each pair of primers (Table 1). Fluorescence was monitored at the end of each extension. Melting curve analysis was added at the end of each amplification cycle. Data analysis was made according to the relative standard curve method. Expression data were reported as the ratio between each investigated cDNA and RPL15 cDNA.

Western Blot

Macrophages were rinsed once in PBS and covered with 80 μL of NuPAGE LDS Sample Buffer 4X (Thermo Fisher

Table 1. *Primers for RT-PCR experiments*

Gene	Primers	Temperature, °C
GLUL	for 5′ TCATCTTGCATCGTGTGTGTG 3′ rev 5′ CTTCAGACCATTCTCCTCCGG 3′	56
SLC38A5	for 5′ AACCTGAGTCTGAGTTGCGG 3′ rev 5′ AGGGAGGGCTCCATTCATCT 3′	57
SLC7A11	for 5′ TGTCCACAAGCACACTCCTC 3′ rev 5′ CTGCCAGCCCCATAAAAAGC 3′	57
SLC38A2	for 5′ ATGAAGAAGGCCGAAATGGGA 3′ rev 5′ TGCTTGGTGGGGTAGGAGTAG 3′	57
SLC3A2	for 5′ TGAATGAGTTAGAGCCCGAGA 3′ rev 5′ GTCTTCCGCCACCTTGATCTT 3′	60
SLC7A5	for 5′ GTGGACTTCGGGAACTATCACC 3′ rev 5′ GAACAGGGACCCATTGACGG 3′	60
GLS	for 5′ GCTGTGCTCCATTGAAGTGA 3′ rev 5′ GCAAACTGCCCTGAGAAGTC 3′	57
TNFA	for 5′ ATGAGCACTGAAAGCATGATCC 3′ rev 5′ GAGGGCTGATTAGAGAGAGGTC 3′	56
RPL-15	for 5′ GCAGCCATCAGGTAAGCCAAG 3′ rev 5′ AGCGGACCCTCAGAAGAAAGC 3′	57

Downloaded from journals.physiology.org/journal/ajpcell at Univ Degli Studi Di Parma Biblio Centrale (160.078.086.043) on September 21, 2026.

Scientific), previously diluted to the working concentration in lysis buffer 1X (Cell Signaling Technology, Milan, Italy). Cell lysates were boiled for 10 min, and protein concentration was determined with the micro-Lowry method. Volumes of lysate corresponding to 20–35 μg of protein were loaded onto 4%–12% polyacrylamide Bolt Bis-Tris Plus Mini Protein Gels (Thermo Fisher Scientific, Milan, Italy), separated at 200 V for 70 min, and then transferred for 1 h to PVDF membranes. After one washing in tris-buffered saline (TBS; 50 mM tris base, 150 mM NaCl, pH 7.5), membranes were incubated for 1 h in TBS containing 10% of blocking solution (Western Blocking Reagent, Roche, Merck, Milan, Italy) before being exposed overnight at 4°C to primary antibodies (Table 2) diluted in TBS-T (TBS with 0.1% Tween) containing 5% BSA. Membranes were then rinsed three times in TBS-T and incubated for 1 h at RT in horseradish peroxidase (HRP)-conjugated secondary anti-mouse or anti-rabbit antibodies (Table 2), both diluted 1:10,000 in blocking solution. After that, membranes underwent three washes of 15 min each with TBS-T before being exposed to ECL Chemiluminescent HRP Substrate (Millipore, Merck, Milan, Italy) for 1 min. Visualization of the protein bands was performed using the iBright FL1500 automated system (Life Technologies, Thermo Fisher Scientific, Milan, Italy). β-actin or β-tubulin were used as a loading control.

Validation of Anti-SNAT5 Antibody Through *SLC38A5* Silencing

Silencing of *SLC38A5* in human macrophages was performed using the HiPerFect Transfection Reagent (Qiagen, Milan, Italy). Mixtures of transfection reagents of either ON-TARGETplus Human SLC38A5 siRNA-SMARTp or scrambled ON-TARGETplus Non-targeting Pool (Horizon Discovery, Cambridge, UK) were used according to the manufacturer's instructions. The experiment (Supplemental Fig. S1) confirmed that *SLC38A5* silencing strongly lowered SNAT5 immunofluorescence.

Immunofluorescence

For staining, macrophages were rinsed twice in PBS and fixed for 15 min with 4% paraformaldehyde in PBS. After two further washes in PBS, fixed cells were permeabilized for 15 min with 0.2% Triton in PBS, blocked for 1 h in PBS containing 2% BSA plus 2% normal goat serum, and incubated overnight at 4°C with mouse anti-human GLUL (1:100), rabbit anti-human glutaminase (GLS, 1:100), or rabbit anti-SNAT5 (1:100) primary antibodies diluted in blocking solution. The specificity of the anti-SNAT5 antibody was also confirmed through the evaluation of SNAT5-silenced macrophages (Supplemental Fig. S1).

After three washes in PBS, cells were incubated for 1 h in the presence of AlexaFluor 488 anti-mouse for GLUL and AlexaFluor 546 anti-rabbit for SNAT5 (both from Thermo Fisher Scientific), diluted 1:400 in blocking solution. For nuclei counterstaining, 1 g/mL of Hoechst 33258 (Merck, Milan, Italy) was added. Slides were then mounted with a coverslide in Glycergel medium (DAKO, Santa Clara, CA) and observed with the confocal laser scanning microscopy (CLSM) system STELLARIS 5 (Leica Microsystems, Wetzlar, Germany), using a Plan-Apo 63× oil immersion objective (numerical aperture 1.4). Single confocal sections were acquired using independent configuration settings to avoid signal cross talk. Setting 1 for nuclei acquisition was excitation at UV 405 nm laser line (LL) and spectral detection ranging from 420 to 468 nm; setting 2 for the detection of GLUL and SNAT5 was, respectively, excitation at 485 nm white laser line (WLL) with a spectral detection range of 500–530 nm and excitation at 549 nm WLL with a spectral detection range of 570–610 nm. Data were analyzed with LAS-X 4.7.0 software.

Transport Studies

The influx of Gln in THP-1 cells and MDM was determined in the absence or in the presence of preferential inhibitors of selected transport systems. Macrophages were washed with Earle's Balanced Salt Solution (EBSS; NaCl 117 mM, KCl 5.3 mM, $CaCl_2$ 1.8 mM, $MgSO_4 \cdot 7H_2O$ 0.81 mM, $NaH_2PO_4 \cdot H_2O$ 1 mM, HEPES 25 mM, glucose 5.5 mM, supplemented with 0.02% phenol red, adjusted to pH 7.4) and incubated in the same solution for 30 min. Cells were then incubated in an EBSS supplemented with 1 mM ^{3}H-Gln (2,3-^{3}H-L-glutamine; PerkinElmer, 10 μCi/mL) for 2 min, with the pH maintained at 7.4 or adjusted at 8.0 with 5 N NaOH, as specified for each experiment, in the absence or in the presence of preferential inhibitors of transporters: L-histidine (His, 10 mM, for system N and system A transporters of the SLC38 family), L-glutamic acid γ-monohydroxamate (GluγHA, 1 mM, for system N transporters of the SLC38 family), or glutamine (Gln, 10 mM, for the inhibition of all the saturable transport systems). Saturable Gln uptake was calculated by subtracting uptake detected in the presence of 10 mM Gln from the uptake values. At the end of the transport assay, cells were washed twice with ice-cold 300 mM urea and extracted in ice-cold ethanol. Radioactivity of the extracts was determined with a MicroBeta2 liquid scintillation spectrometer (PerkinElmer, Milan, Italy). Protein content in the well was determined with a modified Lowry assay. Data were expressed as nmol/mg of protein/min.

Table 2. *Antibodies used for Western blot (WB) and immunofluorescence (IF)*

Antibody	Company Name	Dilution	Source	Cat. No.
ASCT2	Cell Signaling Technology	1:2,000, WB	Rabbit, monoclonal	Cat. No. 8057, RRID:AB_10891440
β-ACTIN	Sigma-Aldrich	1:10,000, WB	Rabbit, polyclonal	Cat. No. A2066, RRID:AB_476693
β-TUBULIN	Sigma-Aldrich	1:10,000, WB	Mouse, monoclonal	Cat. No. T5168, RRID:AB_477579
GLS1	Cell Signaling Technology	1:100, IF	Rabbit, polyclonal	Cat. No. 88964, RRID:AB_2800133
GLUL	BD Biosciences	1:1,000, WB	Mouse, monoclonal	Cat. No. 610518, RRID:AB_39788
SNAT5	Abcam	1:100, IF	Rabbit, polyclonal	Cat. No. ab72717, RRID:AB_10563479
xCT	Abcam	1:1,000, WB	Rabbit, polyclonal	Cat. No. ab37185, RRID:AB_778944

Downloaded from journals.physiology.org/journal/ajpcell at Univ Degli Studi Di Parma Biblio Centrale (160.078.086.043) on September 21, 2026.

Efflux Studies and Amino Acid Determination

Cells were cultured for 24 h in the absence or in the presence of LPS/IFNγ in RPMI 1640 medium at 0.6 mM Gln, 0.137 mM Glu, and 0.208 mM cystine. Cell media was then replaced with fresh medium without Gln (RPMI free-Gln) for further 24 h, maintaining LPS/IFNγ stimulation where required. After the treatment, cells were extracted in absolute ethanol. Amino acids in cell extracts and conditioned media were analyzed with liquid chromatography tandem mass spectrometry (LC-MS/MS). LC analyses were carried out with an ExionLC pump coupled with a QTRAP 6500 + System (SCIEX), as previously described (15).

Statistics

Data are reported as means ± SD of at least three biological replicates. Difference between the experimental conditions was evaluated with a two-tailed, unpaired *t* test, as specified in the figure legends. Differences were considered significant when $P < 0.05$. Statistics were evaluated with Prism 8.0 (GraphPad, La Jolla, CA).

RESULTS

LPS/IFNγ Increase the Expression of Glutamate-Ammonia-Ligase and Gln Transporter SNAT5 in THP-1 Cells

Treatment of differentiated THP-1 macrophages with LPS/IFNγ is associated with M1 polarization, as demonstrated by the early induction of the gene for TNFα (*TNFA*) (Supplemental Fig. S2). Under the same conditions, a substantial change in the expression of genes involved in glutamine (Gln) transport and metabolism was detected (Fig. 1 and Supplemental Fig. S2). Both *GLUL*, for glutamate-ammonia-ligase (GLUL), and *SLC38A5*, for the transporter SNAT5, were significantly induced already after 6 h of LPS/IFNγ stimulation, with a further increase at 24 h (Fig. 1*A*). The induction was confirmed at the protein level for GLUL (Fig. 1*B*).

At the same incubation times, the treatment caused a modest induction of *GLS1*, for the kidney-type glutaminase (Supplemental Fig. S2). Three other transporters for Gln, SNAT2 (*SLC38A2*), ASCT2 (*SLC1A5*), and SNAT7 (*SLC38A7*), were also markedly upregulated but only at 24 h (Supplemental Fig. S2). The treatment with LPS/IFNγ was performed at a [Gln] of 0.6 mM, in the physiological range of plasma Gln, but the enzyme induction was still clearly detectable at the supraphysiological Gln concentration present in most culture media (2 mM) or under conditions of relative (0.4 mM) or absolute (no Gln) depletion of the amino acid (Supplemental Fig. S3). Under the same conditions, induction of ASCT2 by LPS/IFNγ was confirmed at the protein level and found to be insensitive to extracellular Gln deprivation.

Although SNAT5 protein detection with Western blot was not feasible due to the lack of validated antibodies for this technique, M1 macrophages showed an increased expression of both GLUL and SNAT5 with immunofluorescence, which, in addition, highlighted a substantial change in cell

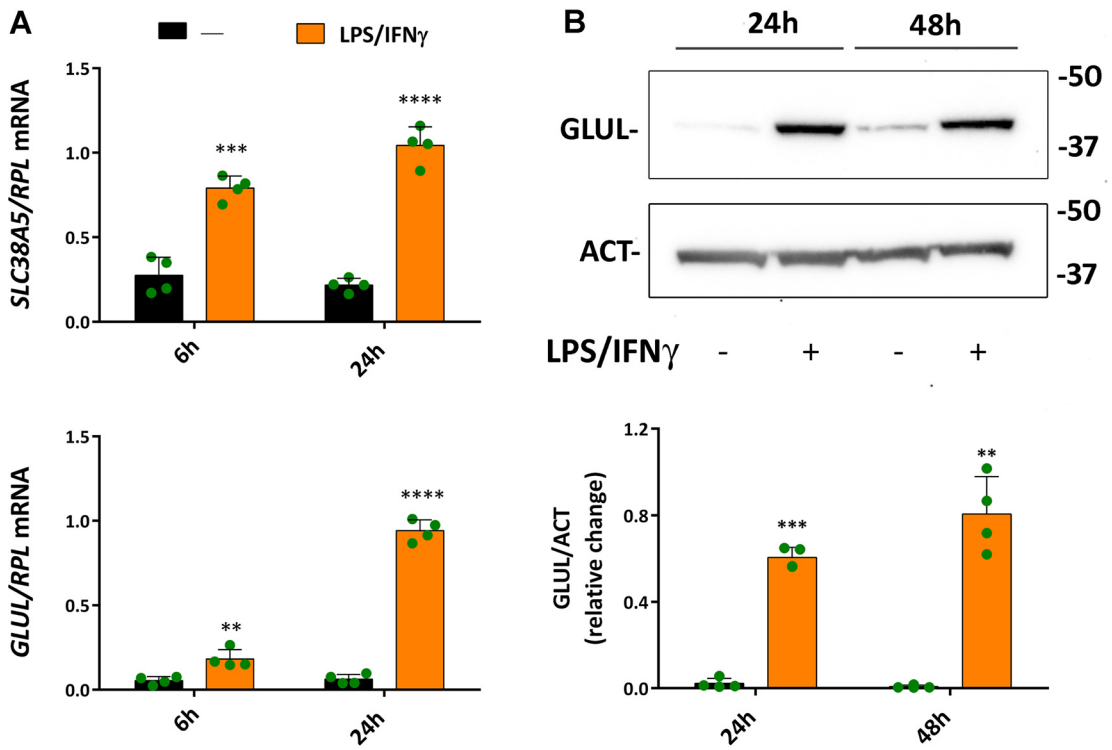


Figure 1. Effect of LPS/IFNγ on GLUL expression. Differentiated THP-1 cells were exposed to LPS/IFNγ for the indicated times and then extracted for the assessment of *GLUL* and *SLC38A5* mRNA (6–24 h, *A*) or of GLUL protein (24–48 h, *B*). A representative Western blot (WB) is reported (*B*, *top*), performed four times with comparable results. The densitometric analysis is shown in *B* (*bottom*). For both panels, data are presented as means of four determinations ± SD ($n = 4$). $^{**}P < 0.01$; $^{***}P < 0.001$; and $^{****}P < 0.0001$ vs. control at the same times; two-tailed, unpaired *t* test. GLUL, glutamate-ammonia-ligase; IFNγ, interferon γ.

Downloaded from journals.physiology.org/journal/ajpcell at Univ Degli Studi Di Parma Biblio Centrale (160.078.086.043) on September 21, 2026.

morphology (Fig. 2). Moreover, several treated cells exhibited evident peripheral localization of SNAT5 signal. Supplemental Fig. S4 compares the intracellular distribution of GLUL and GLS1, showing the uneven cytoplasmic localization of the latter.

M1 Polarization Increases Gln Transport in THP-1 Macrophages

The preferential substrates of the transporter SLC38A5/SNAT5 are Gln, histidine (His), and, with a much lower affinity, asparagine (Asn). In the experiment shown in Fig. 3, the activity of the SNAT5 transporter was evaluated, measuring the saturable Gln influx, which was found markedly stimulated by LPS/IFNγ at both pH 7.4 and 8, a condition in which the operation of the transporter is favored (11). At pH 7.4, His had a modest effect under control conditions, whereas it inhibited almost half of the influx in M1-polarized macrophages. The analog L-glutamate-γ-hydroxamate (GluγHA), which is a synthetic SNAT5 inhibitor (17), was without significant effects in control macrophages, whereas it markedly inhibited Gln entry in cells polarized by LPS/IFNγ. Gln transport was stimulated by LPS/IFNγ also at pH 8.0. Compared with pH 7.4, the inhibition by His was more evident in untreated cells and still marked in M1 macrophages. In the presence of GluγHA, no difference was observed between control and stimulated cells, indicating that the analog completely suppressed the uptake component stimulated by LPS and IFNγ.

The effect of M1 polarization on Gln transport was further characterized by using the preferential inhibitors for other transport systems (Supplemental Fig. S5). In the presence of 10 mM Gln, the transport of the amino acid was comparable

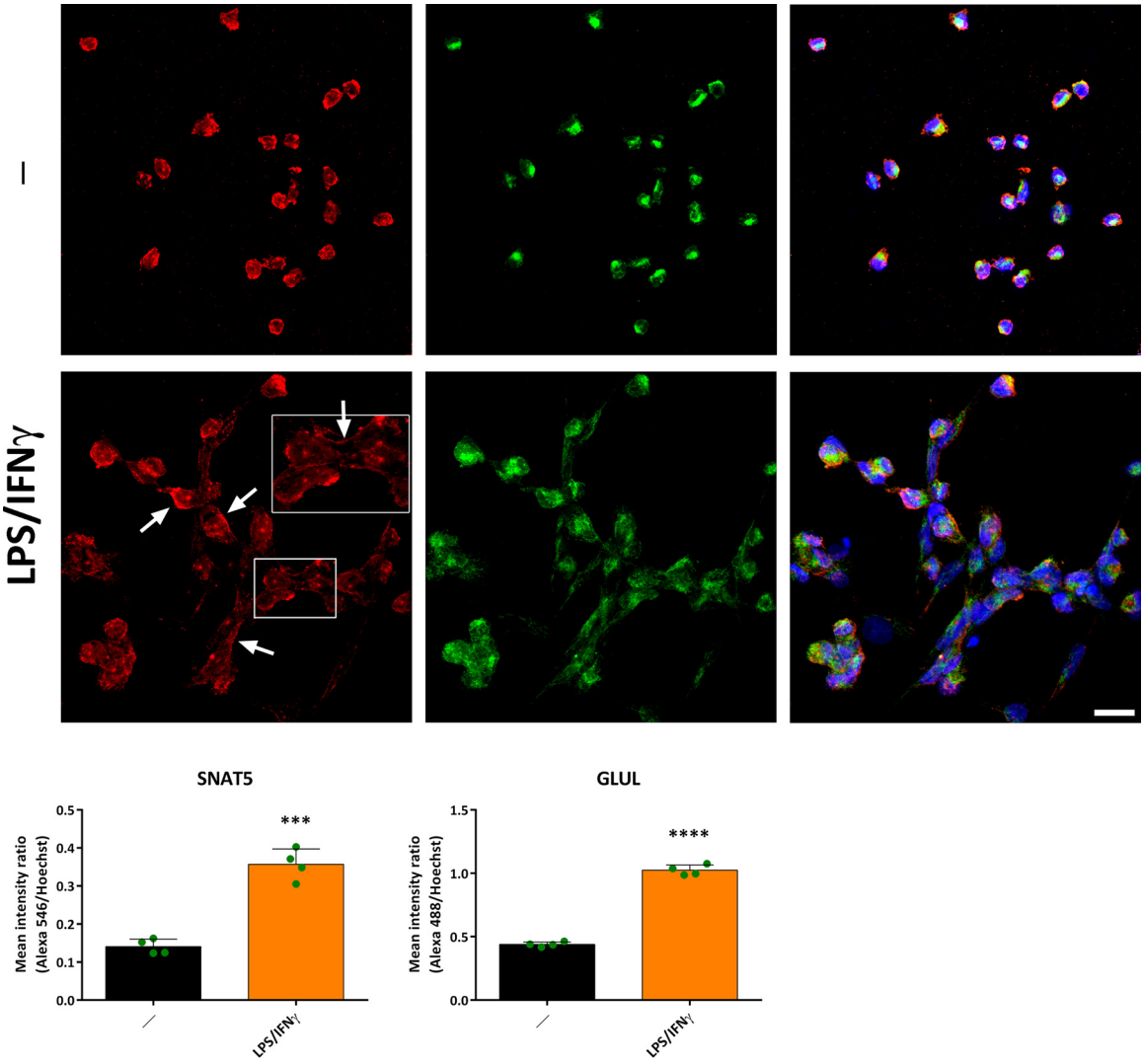


Figure 2. Effect of LPS/IFNγ on SNAT5 and GLUL distribution. THP-1 macrophages were exposed to LPS/IFNγ for 48 h and then processed for SNAT5 and GLUL staining as described in MATERIALS AND METHODS. The images reported are the maximum projection of confocal sections taken in a representative field, highlighting the distribution of SNAT5 (red, *left*) and GLUL (green, *middle*). Arrows indicate areas of marginalization of SNAT5 signal. Nuclei were counterstained with Hoechst 33258 in the merged image. The inset highlights some cells in which membrane localization of SNAT5 is evident. Bar = 50 μm. In the bottom panels, the intensities of SNAT5 and GLUL signals, expressed as ratio on the average of nuclear intensities in the same field, were obtained from four different fields ($n = 4$) and are presented as means ± SD in either experimental condition. ***$P < 0.001$; ****$P < 0.0001$ vs. untreated cells; two-tailed, unpaired *t* test. GLUL, glutamate-ammonia-ligase; IFNγ, interferon γ.

Downloaded from journals.physiology.org/journal/ajpcell at Univ Degli Studi Di Parma Biblio Centrale (160.078.086.043) on September 21, 2026.

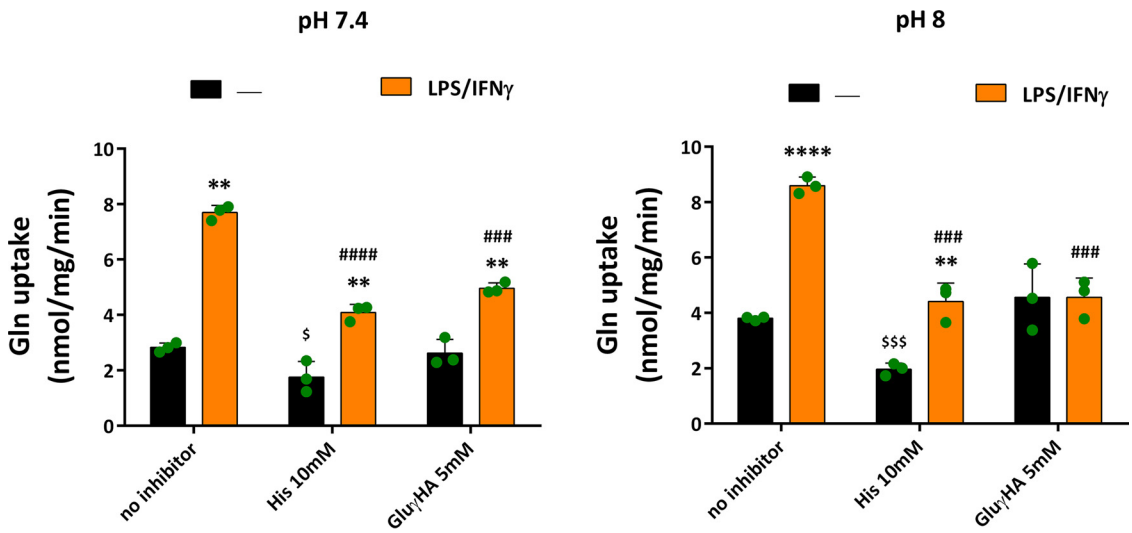


Figure 3. Glutamine influx in LPS/IFNγ-treated or untreated THP-1 cells. After 48 h of LPS/IFNγ treatment, cells were exposed to 1 mM ^{3}H-Gln (10 μCi/mL) for 2 min in EBSS-HEPES at pH 8 or pH 7.4 in the absence or in the presence of the indicated inhibitors. The intracellular content was then extracted and processed for the determination of radiolabeled Gln (see MATERIALS AND METHODS). Data are presented as means of three independent determinations ± SD ($n = 3$). The experiment was performed twice with comparable results. $^{**}P < 0.01$, $^{****}P < 0.0001$ vs. untreated cells under the same conditions of transport assay; $^{\#\#\#}P < 0.001$, $^{\#\#\#\#}P < 0.0001$ vs. LPS/IFNγ-treated cells without inhibitors; $\$P < 0.05$, $\$\$\$P < 0.001$ vs. control cells without inhibitors; two-tailed, unpaired *t* test. EBSS, Earle's Balanced Salt Solution; Gln, glutamine; IFNγ, interferon γ.

in cells polarized by LPS/IFNγ and in control macrophages, indicating that M1 polarization only affected saturable Gln influx. A major component of Gln influx, in both control and M1 macrophages, was threonine-inhibitable, whereas α-(methylamino) isobutyric acid (MeAIB), the specific inhibitor of SNAT1/2 transporters, was ineffective in either experimental condition. Asparagine at high concentration markedly inhibited Gln influx in both cells, suppressing the stimulation.

M1 Polarization Does Not Change Intracellular Gln but Enhances the Efflux of Gln and Glu

Since SNAT5 is a bidirectional transporter (11), its late induction in M1-polarized macrophages may lead to the increase of either Gln influx or efflux. Moreover, the exchange transporter ASCT2 and two important Gln-related enzymes with opposite effects on Gln cell content, glutamate-ammonia-ligase and glutaminase, are also induced by LPS/IFNγ (Fig. 1 and Supplemental Fig. S2). Therefore, to evaluate the net effect of these changes, we have determined the cell content and the extracellular concentration of Gln, together with those of its main metabolite L-glutamate (Glu) (Figs. 4 and 5).

Upon 24 h of incubation at 0.6 mM Gln, the intracellular amount of Gln (Fig. 4*A*) was not significantly different in control and M1 macrophages. After further 24 h of incubation in a Gln-free medium, cell Gln was much lower but still comparable under the two conditions, whereas the extracellular amino acid was markedly higher in M1-polarized cultures (Fig. 4*B*), indicating a threefold higher efflux (Fig. 4*C*). The sum of intra- and extracellular amino acid indicated that the treatment increased total Gln content of the culture by 50% (Fig. 4*D*).

In addition, cell Glu (Fig. 5*A*) was comparable in M0 and M1 macrophages, although Gln-free incubation produced a marked decrease in both conditions. The extracellular Glu concentration was much higher in LPS/IFNγ-treated cells (Fig. 5*B*) and, importantly, higher than the initial medium concentration (137 μM) in both M0 and M1 macrophage cultures. Therefore, a net Glu efflux had occurred in either case, which was 2.4-fold higher in M1-polarized macrophages (Fig. 5*C*). Total Glu content of the culture system was not significantly different under the two conditions.

M1 Polarization Induces the Transporter xCT

In several cell models, Glu efflux is mediated by the transporter xCT, an anionic amino acid exchanger that, under physiological conditions, operates cystine influx coupled with Glu efflux (18–20). An increased expression of *SLC7A11*, coding for xCT, was detected in LPS/IFNγ-stimulated THP-1 cells at 6 h and, more evidently, at 24 h of treatment. Gene induction was followed by increased abundance of the carrier protein at 24 and 48 h (Fig. 6). Consistently, the xCT inhibitor sulfasalazine significantly lowered extracellular Glu in LPS/IFNγ-treated but not in control cells (Supplemental Fig. S6).

LPS/IFNγ Treatment Promotes Both *GLUL* and *SLC38A5* Expression in Primary Human Macrophages

A 24-h incubation with LPS/IFNγ markedly stimulated *SLC38A5*, *GLUL*, and *SLC7A11* expression in human primary macrophages derived from peripheral blood monocytes (MDM) (Fig. 7, *A–C*). At 48 h of treatment, Gln transport was increased in M1-polarized macrophages with the stimulation abolished by high concentrations of the SNAT5 inhibitors His and GluγHA. Consistently, a significant increase in SNAT5 protein expression on the plasma membrane of M1-polarized MDM was observed (Fig. 8).

Downloaded from journals.physiology.org/journal/ajpcell at Univ Degli Studi Di Parma Biblio Centrale (160.078.086.043) on September 21, 2026.

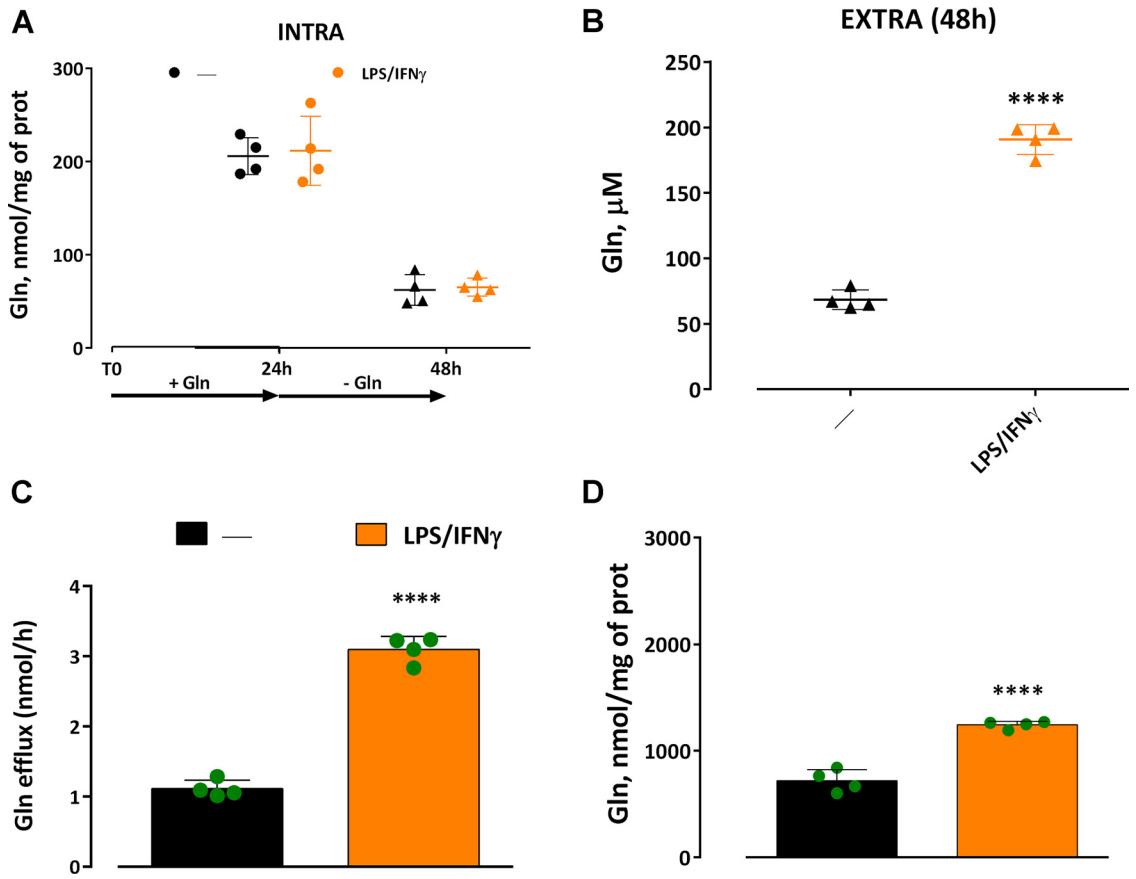


Figure 4. Intracellular and extracellular Gln upon LPS/IFNγ treatment. Cells were incubated 24 h in the absence or presence of LPS/IFNγ. The incubation was prolonged for further 24 h in the absence of Gln, maintaining the stimulation where indicated. After the experimental treatment, cell culture media were collected and stored at −80°C along with the intracellular contents extracted in ethanol. Gln was determined in the two fractions with LC-MS/MS (see MATERIALS AND METHODS). For intracellular amino acid (*A*), data at 24 and 48 h are normalized for the cell protein of the same well. Extracellular amino acid (*B*) is expressed as Gln concentration. In *C*, the extracellular concentrations (*B*) has been converted into the amount of amino acid secreted by cells and expressed as efflux (nmol/h). *D*: represents the total amount of Gln in the culture system, summing cell Gln and the extracellular amino acid obtained from the concentration corrected for the incubation volume. For all panels, results are means of four independent determinations ± SD ($n = 4$). ****$P <$ 0.0001 vs. untreated cells; two-tailed, unpaired *t* test. Gln, glutamine; IFNγ, interferon γ; LC-MS/MS, liquid chromatography tandem mass spectrometry.

DISCUSSION

This study demonstrates that M1 polarization of human macrophages promotes the intracellular synthesis of Gln through glutamine synthetase (GLUL) and enhances Gln efflux into the extracellular medium.

As far as GLUL is concerned, previous studies from this laboratory (5) found that the enzyme was induced by LPS. Others demonstrated that GLUL induction was also observed with the combined treatment with LPS/IFNγ (6), ascribing the regulation to a metabolic rewiring associated with M2 polarization. It is known, however, that M2 macrophages activate glutamine catabolism and that glutamine deprivation hampered M2 polarization (21). It should be considered that the metabolic changes associated with M1-like phenotype, such as activation of glycolytic flux, occur early after exposure to pathogens (22, 23). In the present work, GLUL expression has been investigated at 24 and 48 h of LPS/IFNγ, M1 mimicking treatment, when the metabolic phenotype may represent a transitional state toward M2 polarization, as suggested by Jiang et al. (3). Following macrophage activation for an extended period, a biphasic change can be indeed detected (24), with M1 metabolic phenotype prevailing in the early phases with a later shift toward M2. If this is true, GLUL induction could be a marker of the metabolic shift from M1 to M2 metabolic phenotype.

GLUL regulation may involve transcriptional (through *GLUL* induction) and posttranslational mechanisms, with GLUL shelf life inversely dependent on Gln availability (25, 26). In our experiments, the transcriptional activation of *GLUL* was evident, but we also considered the other mechanism (Supplemental Fig. S3). At 2 mM, the Gln concentration usually adopted in conventional media, GLUL protein expression was suppressed in control cells, with a dramatic induction upon LPS/IFNγ treatment. Instead, at the physiological extracellular concentration of 0.6 mM, the expression in control cells was already sizable, although LPS/IFNγ stimulation was still clear (Supplemental Fig. S3). Therefore, to better adhere to the physiological situation, we performed macrophage activation at 0.6 mM Gln.

At variance with GLUL regulation, the role of changes in Gln transport in M1 polarization of human macrophages has not been thoroughly investigated thus far. The results presented here indicate, however, that Gln transport is

Downloaded from journals.physiology.org/journal/ajpcell at Univ Degli Studi Di Parma Biblio Centrale (160.078.086.043) on September 21, 2026.

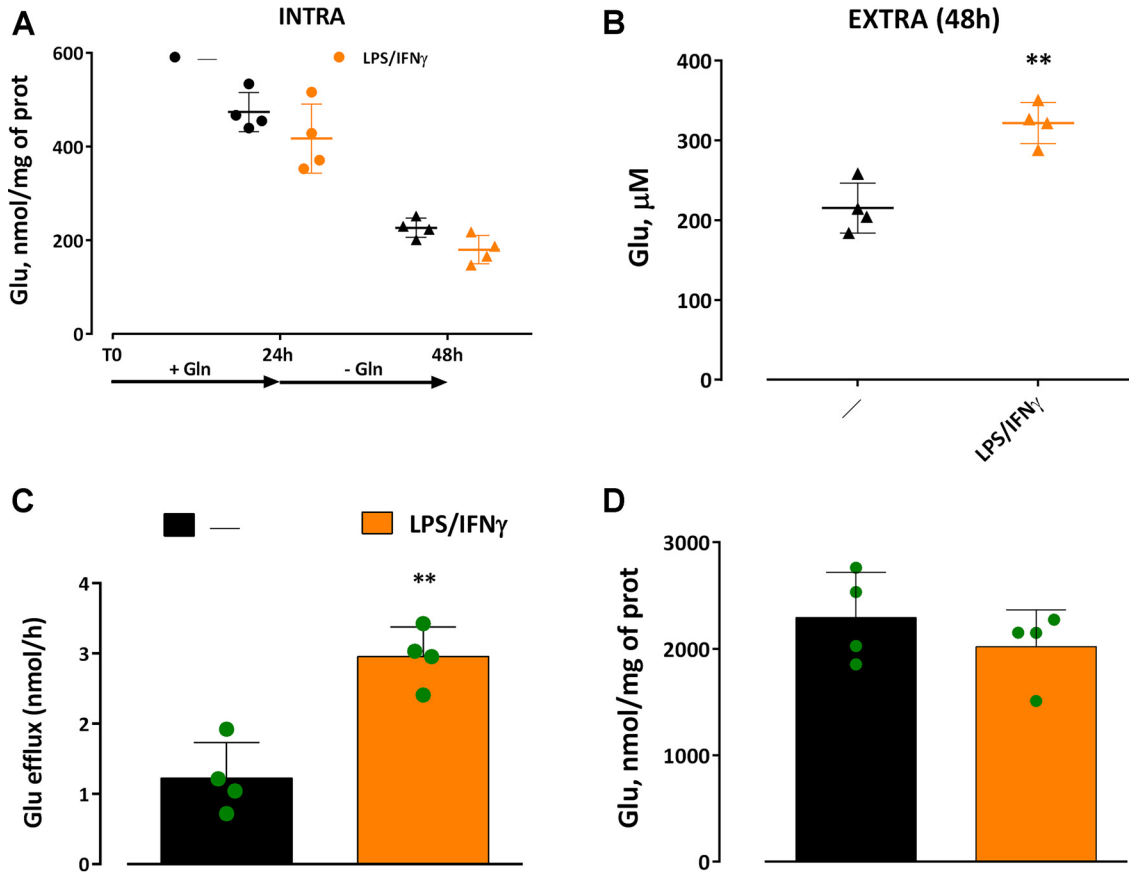


Figure 5. Intracellular and extracellular Glu upon LPS/IFNγ treatment. Glu was measured under the same conditions described in the legend of Fig. 4. Data were expressed and panels were defined as described in the legend of Fig. 4. In *C*, the medium Glu concentration (137 µM) was subtracted from the extracellular concentration before efflux calculation. For all panels, results are means of four independent determinations ± SD ($n = 4$). $^{**}P < 0.01$ vs. untreated cells; two-tailed, unpaired *t* test. Glu, glutamate; IFNγ, interferon γ.

markedly increased at later times of M1 polarization (Figs. 4 and 7). Looking at the transporter(s) responsible for the change, we observed a significant induction of *SLC38A2*/SNAT2 at 24 h of treatment with LPS/IFNγ (Supplemental Fig. S2), but MeAIB inhibition is very low in both control and M1-polarized THP-1 cells (Supplemental Fig. S5). SNAT2 is regulated at many levels, and changes in *SLC38A2* expression are not always followed by membrane targeting of the carrier and increase in transport activity (27). *SLC1A5*/ASCT2 is considered the major Gln transporter of macrophages, and its inhibition has been proposed as an effective anti-inflammatory strategy (28). Consistently, ASCT2 seems to play a leading role in Gln transport also in THP1 cells, since its preferential substrate L-threonine exerts a marked inhibition (Supplemental Fig. S5). The transporter is strongly induced by LPS/IFNγ at the gene (Supplemental Fig. S2) and protein level (Supplemental Fig. S3). Gln is also a substrate of system N, which includes bidirectional SNAT transporters. One of these transporters, SNAT5, also interacts with L-threonine (29), at variance with its homologous SNAT3 (11). In agreement with SNAT5 involvement, the M1-dependent stimulation of Gln transport is markedly lowered by the system N inhibitors His and γ-glutamylhydroxamate (GluγHA) at pH 7.4 and completely suppressed at pH 8, a condition in which system N activity is stimulated (30, 31). Among system N transporters (11), *SLC38A5*/SNAT5 is clearly induced during M1 polarization (Figs. 1 and 2), whereas SNAT3 expression is exceedingly low (data not shown). SNAT7 is sizably expressed in macrophages and appreciably induced by LPS/IFNγ (Supplemental Fig. S2) but prevalently localized in intracellular compartments (11). For these reasons we conclude that the system N transporter responsible for increased Gln transport in M1-polarized THP-1 cells is SNAT5.

Therefore, M1 polarization induces at least two transporters that may account for Gln efflux, such as ASCT2 and SNAT5. However, the operational conditions and the pH dependence of the two carriers are different. ASCT2 is an obligatory Na^+-dependent exchanger and is inhibited by alkalinization, whereas SNAT5 mediates a Na^+-dependent unidirectional influx stimulated at pH 8. The experiment shown in Fig. 3 indicates that the preferential SNAT5 inhibitor GluγHA does not completely suppress Gln transport stimulation at pH 7.4, when the activity of ASCT2 is optimal, but it abolishes stimulation at pH 8, when SNAT5-dependent influx is promoted and ASCT2 is hindered (32). These results suggest that both transporters contribute to the stimulation of Gln efflux, with the relative contribution depending on the availability of counter substrates for ASCT2 and the transmembrane gradient of Gln and pH for SNAT5. Interestingly, it is known that M1-activation produces a

Downloaded from journals.physiology.org/journal/ajpcell at Univ Degli Studi Di Parma Biblio Centrale (160.078.086.043) on September 21, 2026.

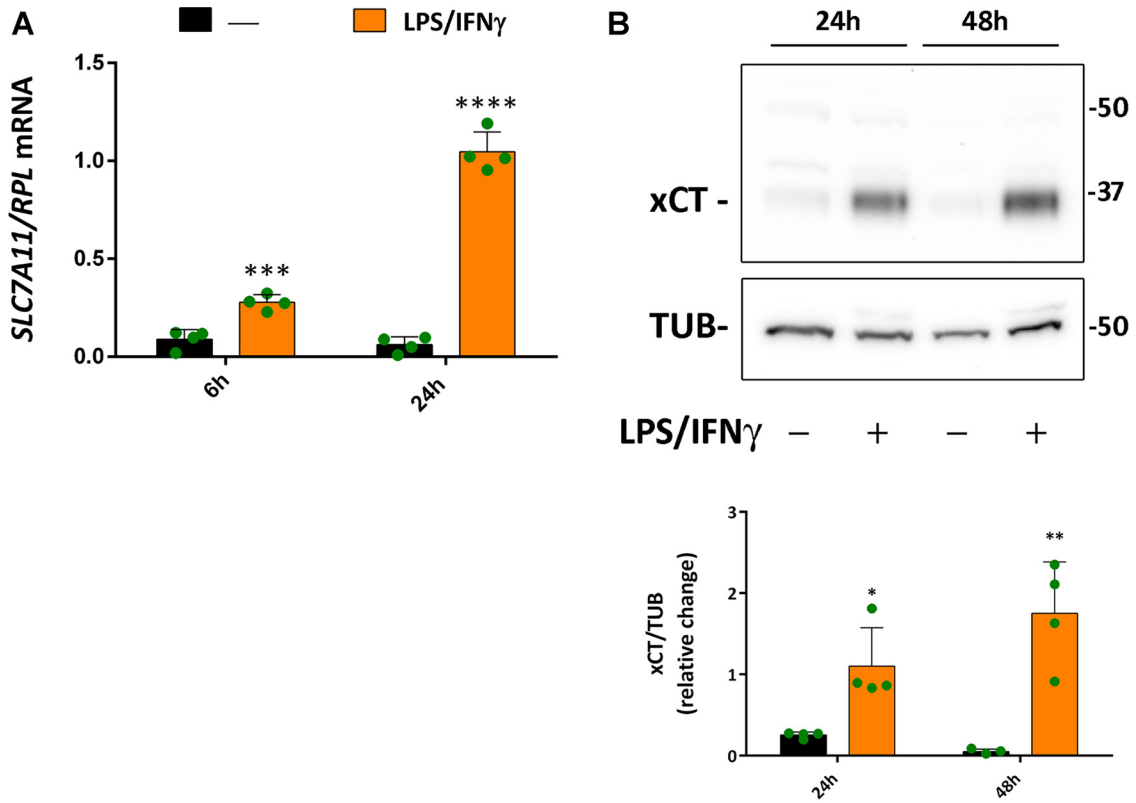


Figure 6. LPS/IFNγ effect on xCT transporter in THP-1 macrophages. Differentiated THP-1 cells were exposed to LPS/IFNγ for the indicated times. mRNA (*A*) and proteins (*B*) were analyzed for SLC7A11/xCT expression. A representative WB is reported (*B*, *top*), with densitometric analysis shown in *B* (*bottom*). For both panels, data are presented as means of four independent determinations ± SD ($n = 4$). *$P < 0.05$; **$P < 0.01$, ***$P < 0.001$; ****$P < 0.0001$ vs. untreated cells; two-tailed, unpaired *t* test. IFNγ, interferon γ.

significant decrease of extracellular pH (33), a condition that should promote SNAT5-mediated Gln efflux. This consideration could be particularly relevant in specific pathological situations associated with low pH, such as inflammatory infiltrates and tumor microenvironment. On the contrary, the experiment shown in Fig. 4 has been performed in the absence of extracellular Gln to highlight different rates of efflux in control and M1-polarized cells. Under this condition, the contribution of ASCT2 to Gln efflux is expected to be emphasized due to lack of competition with other ASCT2 substrate for influx. However, in a real-life situation, extracellular Gln would be present, so that the net contribution of ASCT2 to Gln efflux would be less evident. These possibilities require experimental validation in advanced culture systems.

The function of this bidirectional transporter has never been specifically investigated in M1 human macrophages, and no information is yet available on its role in the metabolic changes related to M1 polarization. In Protein Atlas, the gene is not considered appreciably expressed in cells of the monocyte-macrophage lineage (34), but these data refer to unstimulated cells. Instead, previous results indicated that a strong induction of the gene occurs upon the activation of human macrophages by LPS (35, 36). However, both these papers reported the change of transporter expression at mRNA level in the context of a genome-wide transcriptomic analysis, and the effect was neither described in the text nor involved in functional changes. Here, we demonstrate that the transporter is markedly induced in a typical M1-polarizing condition and that, upon its induction, Gln transport markedly changes, suggesting that SNAT5 induction has a functional role. Both *GLUL* and *SLC38A5* are induced, indicating that macrophages treated with LPS/IFNγ increase both the synthesis of Gln and its transmembrane fluxes. Moreover, glutaminase, the major Gln-catabolizing enzyme, and two other Gln transporters, SNAT2 and ASCT2, are also induced under the same conditions (Supplemental Figs. S2 and S3). Therefore, the overall effect of these changes on cell Gln would be hardly predictable.

Measuring both intracellular and extracellular Gln (Fig. 4), we found that the overall functional outcome of M1-associated changes is the increased extrusion of the amino acid. Indeed, upon a Gln-free incubation of 24 h, the extracellular concentration of the amino acid was markedly higher in M1-polarized than in control cultures (Fig. 4*B*), corresponding to a threefold increased efflux (Fig. 4*C*). Nevertheless, the intracellular content of Gln was not different in control and treated cells (Fig. 4*A*), independently of substantial changes in single enzymes or transporters induced by inflammatory stimuli. This paradoxical finding can be explained only by GLUL-dependent synthesis of Gln, given the absence of extracellular amino acid. Gln plays several roles in cell metabolism, including anaplerosis, nucleotide synthesis, synthesis of glutamate and asparagine (directly) and of other nonessential amino acids (through glutamine-derived glutamate), synthesis of hexosamines, prevention of

Downloaded from journals.physiology.org/journal/ajpcell at Univ Degli Studi Di Parma Biblio Centrale (160.078.086.043) on September 21, 2026.

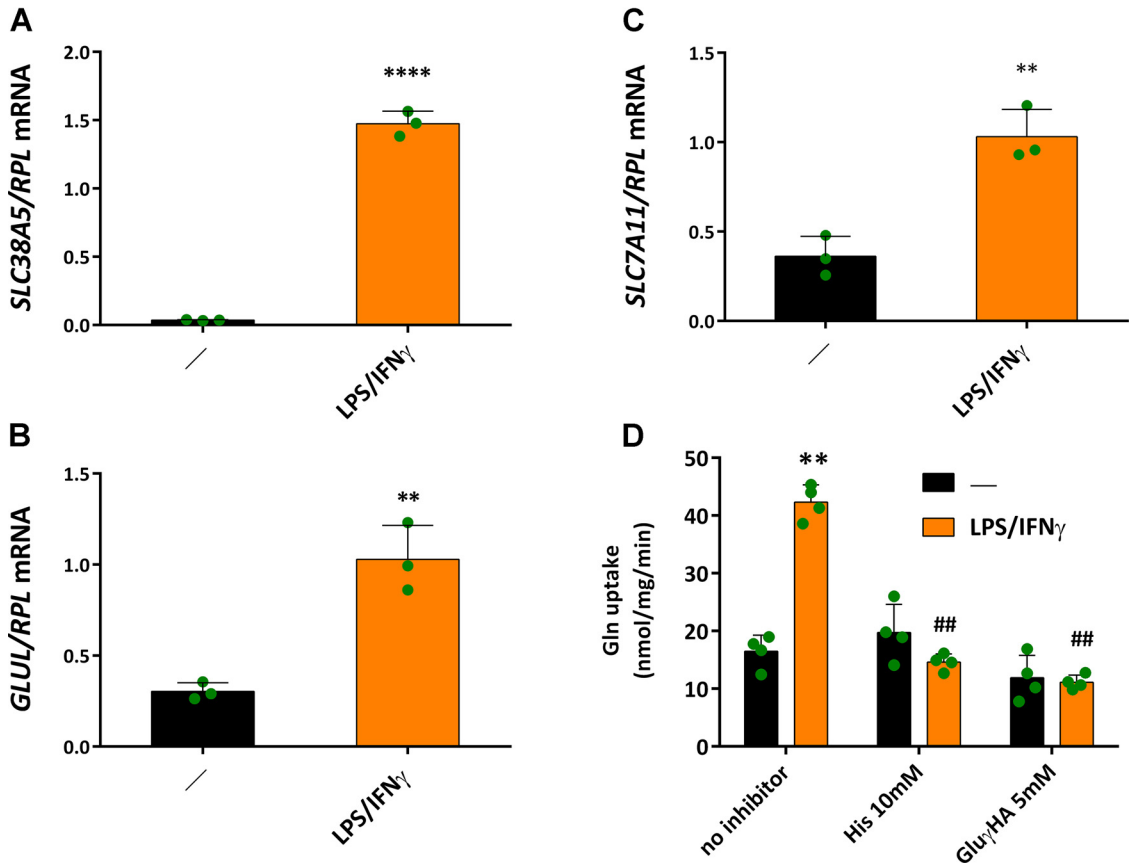


Figure 7. LPS/IFNγ effects on primary human macrophages. Differentiated primary human macrophages from peripheral blood monocytes were exposed to LPS (5 ng/mL)/IFNγ (20 ng/mL) for 24 (*A*–*C*) or 48 h (*D*). *A*–*C*: the expression of *SLC38A5* (*A*), *GLUL* (*B*), and *SLC7A11* (*C*) was determined at 24 h. *D*: the saturable transport of ^{3}H-Gln (1 mM, 10 μCi/mL, 2 min, pH 8) was determined after 48 h of treatment in the presence or in the absence of the indicated inhibitors. Data are presented as means of three (*A*–*C*, $n = 3$) or four (*D*, $n = 4$) independent determinations ± SD. $^{**}P < 0.01$, $^{****}P < 0.0001$ vs. untreated cells; $\#\#P < 0.01$, vs. LPS/IFNγ-treated cells without inhibitors; two-tailed, unpaired *t* test. GLUL, glutamate-ammonia-ligase; IFNγ, interferon γ.

oxidative stress, and control of cell volume. An unbalanced change in Gln content, associated with different functional states, may have profound consequences for cell homeostasis, thus highlighting the importance of an overall equilibrium among changes of different Gln enzymes and transporters.

Similarly to the homolog SNAT3, SNAT5 engages in Gln efflux from glial cells (37). More recently, the transporter has been repeatedly indicated as the efflux route for the typical system N substrates, Gln and Asn, to sustain amino acid cross talks between different cell types (14). For instance, bone marrow mesenchymal stromal cells exploit SNAT5 transporter to internalize Gln, in particular under hypoxic conditions (38), but at the same time to mediate asparagine efflux and metabolic support to acute lymphoblastic leukemia blasts (39). Similarly, in multiple myeloma bone marrow niche, mesenchymal cells are driven to use the transporter to mediate Gln efflux that is then used by GLUL-negative myeloma plasma cells (40). Most recently, it has been shown that glutamine produced by M2 macrophages is taken up by oral squamous carcinoma cells through SLC38A5, although the transport system for Gln secretion by macrophages was not identified (41). As far as nontumor models are concerned, GLUL-dependent secretion of Gln from macrophages has been proposed to play an important role in muscle regeneration (42). However, in that contribution, the efflux route exploited to secrete the amino acid was not investigated.

Glutamate (Glu) is the primary metabolite of Gln in many cell types. Although Glu is present in the medium, Glu content of THP-1 cells markedly fell after Gln-free incubation (Fig. 3), suggesting that a substantial quote of the amino acid derives from extracellular Gln. The extracellular concentration of the anionic amino acid was much higher in cultures treated with LPS/IFNγ, highlighting an increased efflux, attributable to the cystine/Glu exchanger xCT, induced by the same treatment (Fig. 6). Upregulation of xCT/*SLC7A11* by inflammatory stimuli is a well-known feature of the transporter (18), although evidence in human macrophages is limited (43). In our hands, the induction of *SLC7A11* was associated with that of its chaperone *SLC3A2* (Supplemental Fig. S2). This regulation has been usually associated with the cell response to oxidative stress and implied in contrast to ferroptosis through the Glu-dependent influx of cystine (44). The stimulation of Glu efflux increased the extracellular concentration of the anionic amino acid well over the level present in the medium (138 μM; Fig. 5*B*).

Downloaded from journals.physiology.org/journal/ajpcell at Univ Degli Studi Di Parma Biblio Centrale (160.078.086.043) on September 21, 2026.

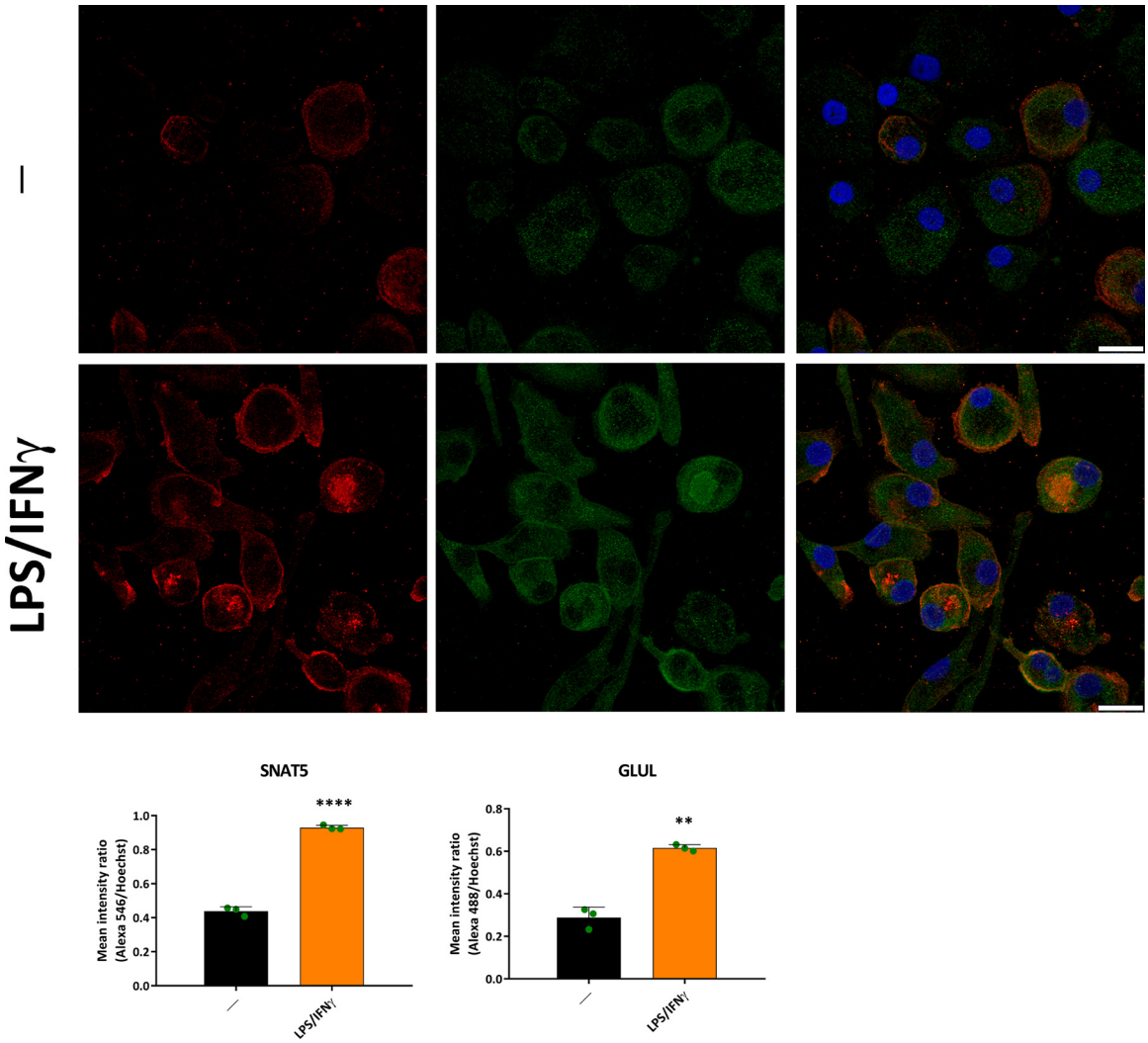


Figure 8. Effect of LPS/IFNγ on SNAT5 and GLUL distribution in primary human macrophages. Macrophages were exposed to LPS/IFNγ for 48 h and then processed for SNAT5 and GLUL staining as described in MATERIALS AND METHODS. The images reported are the maximum projection of confocal sections taken in a representative field, highlighting the distribution of SNAT5 (red, *left*) and GLUL (green, *middle*). Nuclei were counterstained with Hoechst 33258 in the merged image. Bar = 20 μm. In the bottom panels, the intensities of SNAT5 and GLUL signals, expressed as a ratio to the average of nuclear intensities in the same field, were obtained from three different fields ($n = 3$) and are presented as means ± SD in either experimental condition. $^{**}P < 0.01$; $^{****}P < 0.0001$ vs. untreated cells; two-tailed, unpaired *t* test. GLUL, glutamate-ammonia-ligase; IFNγ, interferon γ.

The physiological relevance of these findings is strengthened by the demonstration that primary human MDM also induce *GLUL*, *SLC38A5*, and *SLC7A11* at late times of M1 polarization induced by LPS/IFNγ. In conclusion, these results suggest that M1-polarized human macrophages can modify the extracellular concentrations of both Gln and Glu, thus potentially influencing the behavior of other cells present in the immune microenvironment. The implications of this hypothesis in real-life contexts, such as immune, inflammatory, or tumor microenvironments, will require further experiments in coculture or in vivo models.

DATA AVAILABILITY

The data that support the findings of this study are available in MATERIALS AND METHODS and RESULTS of the article. Raw data are available from the corresponding authors upon request.

SUPPLEMENTAL MATERIAL

Supplemental Figs. S1–S6: https://doi.org/10.6084/m9.figshare.33121259.

ACKNOWLEDGMENTS

The equipment for the liquid chromatography coupled with mass spectrometry experiments was partly supported by the University of Parma through the Scientific Instrumentation Upgrade Program 2018. The confocal experiments were conducted at the Confocal Microscopy Laboratory (Department of Medicine and Surgery, University of Parma). The cost of the Leica STELLARIS 5 confocal system used for this experimental investigation was partly supported by the University of Parma through the Scientific Instrumentation Upgrade Program 2019.

Graphical abstract created with a licensed version of BioRender.com.

Downloaded from journals.physiology.org/journal/ajpcell at Univ Degli Studi Di Parma Biblio Centrale (160.078.086.043) on September 21, 2026.

GRANTS

This work has been supported by the University of Parma through Action B, Bando di Ateneo per la Ricerca 2025 (to M.G.B. and M.C.) and Action A, Bando di Ateneo per la Ricerca 2024 (to O.B.). G.T. is supported by Fondazione AIRC per la ricerca sul cancro ETS (AIRC).

DISCLOSURES

No conflicts of interest, financial or otherwise, are declared by the authors.

AUTHOR CONTRIBUTIONS

M.G.B. conceived and designed research; G.T., M.C., C.U., C.M., R.A., G.L., and M.G.B. performed experiments; G.T., M.C., C.U., C.M., R.A., G.L., and M.G.B. analyzed data; G.T., M.C., C.U., C.M., R.A., G.L., and M.G.B. interpreted results of experiments; M.G.B. prepared figures; M.G.B. drafted manuscript; M.V., O.B., and M.G.B. edited and revised manuscript; G.T., M.C., C.U., C.M., R.A., G.L., M.V., O.B., and M.G.B. approved final version of manuscript.

REFERENCES

1. **Biswas SK**, **Mantovani A.** Orchestration of metabolism by macrophages. *Cell Metab* 15: 432–437, 2012. doi:10.1016/j.cmet.2011.11.013.
2. **Curi R**, **de Siqueira Mendes R**, **de Campos Crispin LA**, **Norata GD**, **Sampaio SC**, **Newsholme P.** A past and present overview of macrophage metabolism and functional outcomes. *Clin Sci (Lond)* 131: 1329–1342, 2017. doi:10.1042/CS20170220.
3. **Jiang Q**, **Qiu Y**, **Kurland IJ**, **Drlica K**, **Subbian S**, **Tyagi S**, **Shi L.** Glutamine is required for m1-like polarization of macrophages in response to *Mycobacterium tuberculosis* infection. *mBio* 13: e0127422, 2022. doi:10.1128/mbio.01274-22.
4. **Bianchi MG**, **Chiu M**, **Taurino G**, **Bergamaschi E**, **Cubadda F**, **Macaluso GM**, **Bussolati O.** The TLR4/NFκB-dependent inflammatory response activated by LPS is inhibited in human macrophages pre-exposed to amorphous silica nanoparticles. *Nanomaterials (Basel)* 12: 2307, 2022. doi:10.3390/nano12132307.
5. **Bianchi MG**, **Chiu M**, **Taurino G**, **Ruotolo R**, **Marmiroli N**, **Bergamaschi E**, **Cubadda F**, **Bussolati O.** Pyrogenic and precipitated amorphous silica nanoparticles differentially affect cell responses to LPS in human macrophages. *Nanomaterials (Basel)* 10: 1395, 2020. doi:10.3390/nano10071395.
6. **Palmieri EM**, **Menga A**, **Martin-Perez R**, **Quinto A**, **Riera-Domingo C**, **De Tullio G**, **Hooper DC**, **Lamers WH**, **Ghesquiere B**, **McVicar DW**, **Guarini A**, **Mazzone M**, **Castegna A.** Pharmacologic or genetic targeting of glutamine synthetase skews macrophages toward an M1-like phenotype and inhibits tumor metastasis. *Cell Rep* 20: 1654–1666, 2017. doi:10.1016/j.celrep.2017.07.054.
7. **Nguyen TV**, **Lee JE**, **Sweredoski MJ**, **Yang SJ**, **Jeon SJ**, **Harrison JS**, **Yim JH**, **Lee SG**, **Handa H**, **Kuhlman B**, **Jeong JS**, **Reitsma JM**, **Park CS**, **Hess S**, **Deshaies RJ.** Glutamine triggers acetylation-dependent degradation of glutamine synthetase via the thalidomide receptor cereblon. *Mol Cell* 61: 809–820, 2016. doi:10.1016/j.molcel.2016.02.032.
8. **Kandasamy P**, **Gyimesi G**, **Kanai Y**, **Hediger MA.** Amino acid transporters revisited: new views in health and disease. *Trends Biochem Sci* 43: 752–789, 2018. doi:10.1016/j.tibs.2018.05.003.
9. **Bhutia YD**, **Ganapathy V.** Glutamine transporters in mammalian cells and their functions in physiology and cancer. *Biochim Biophys Acta* 1863: 2531–2539, 2016. doi:10.1016/j.bbamcr.2015.12.017.
10. **Cheng X**, **Wang Y**, **Gong G**, **Shen P**, **Li Z**, **Bian J.** Design strategies and recent development of bioactive modulators for glutamine transporters. *Drug Discov Today* 29: 103880, 2024. doi:10.1016/j.drudis.2024.103880.
11. **Broer S.** The SLC38 family of sodium-amino acid co-transporters. *Pflugers Arch* 466: 155–172, 2014. doi:10.1007/s00424-013-1393-y.
12. **Kanai Y**, **Hediger MA.** The glutamate/neutral amino acid transporter family SLC1: molecular, physiological and pharmacological aspects. *Pflugers Arch* 447: 469–479, 2004. doi:10.1007/s00424-003-1146-4.
13. **Mackenzie B**, **Erickson JD.** Sodium-coupled neutral amino acid (System N/A) transporters of the SLC38 gene family. *Pflugers Arch* 447: 784–795, 2004. doi:10.1007/s00424-003-1117-9.
14. **Taurino G**, **Chiu M**, **Bianchi MG**, **Griffini E**, **Bussolati O.** The SLC38A5/SNAT5 amino acid transporter: from pathophysiology to pro-cancer roles in the tumor microenvironment. *Am J Physiol Cell Physiol* 325: C550–C562, 2023. doi:10.1152/ajpcell.00169.2023.
15. **Taurino G**, **Dander E**, **Chiu M**, **Pozzi G**, **Maccari C**, **Starace R**, **Silvestri D**, **Griffini E**, **Bianchi MG**, **Carubbi C**, **Andreoli R**, **Mirandola P**, **Valsecchi MG**, **Rizzari C**, **D'Amico G**, **Bussolati O.** Asparagine transport through SLC1A5/ASCT2 and SLC38A5/SNAT5 is essential for BCP-ALL cell survival and a potential therapeutic target. *Br J Haematol* 205: 175–188, 2024. doi:10.1111/bjh.19516.
16. **Balkrishna S**, **Broer A**, **Welford SM**, **Hatzoglou M**, **Broer S.** Expression of glutamine transporter Slc38a3 (SNAT3) during acidosis is mediated by a different mechanism than tissue-specific expression. *Cell Physiol Biochem* 33: 1591–1606, 2014. doi:10.1159/000358722.
17. **Hashim M**, **Yokoi N**, **Takahashi H**, **Gheni G**, **Okechi OS**, **Hayami T**, **Murao N**, **Hidaka S**, **Minami K**, **Mizoguchi A**, **Seino S.** Inhibition of SNAT5 induces incretin-responsive state from incretin-unresponsive state in pancreatic beta-cells: study of beta-cell spheroid clusters as a model. *Diabetes* 67: 1795–1806, 2018. doi:10.2337/db17-1486.
18. **Verrey F**, **Closs EI**, **Wagner CA**, **Palacin M**, **Endou H**, **Kanai Y.** CATs and HATs: the SLC7 family of amino acid transporters. *Pflugers Arch* 447: 532–542, 2004. doi:10.1007/s00424-003-1086-z.
19. **Rimaniol AC**, **Mialocq P**, **Clayette P**, **Dormont D**, **Gras G.** Role of glutamate transporters in the regulation of glutathione levels in human macrophages. *Am J Physiol Cell Physiol* 281: C1964–C1970, 2001. doi:10.1152/ajpcell.2001.281.6.C1964.
20. **Salti T**, **Braunstein I**, **Haimovich Y**, **Ziv T**, **Benhar M.** Widespread S-persulfidation in activated macrophages as a protective mechanism against oxidative-inflammatory stress. *Redox Biol* 72: 103125, 2024. doi:10.1016/j.redox.2024.103125.
21. **Jha AK**, **Huang SC**, **Sergushichev A**, **Lampropoulou V**, **Ivanova Y**, **Loginicheva E**, **Chmielewski K**, **Stewart KM**, **Ashall J**, **Everts B**, **Pearce EJ**, **Driggers EM**, **Artyomov MN.** Network integration of parallel metabolic and transcriptional data reveals metabolic modules that regulate macrophage polarization. *Immunity* 42: 419–430, 2015. doi:10.1016/j.immuni.2015.02.005.
22. **Koo SJ**, **Chowdhury IH**, **Szczesny B**, **Wan X**, **Garg NJ.** Macrophages promote oxidative metabolism to drive nitric oxide generation in response to *Trypanosoma cruzi*. *Infect Immun* 84: 3527–3541, 2016. doi:10.1128/IAI.00809-16.
23. **Roy S**, **Schmeier S**, **Kaczkowski B**, **Arner E**, **Alam T**, **Ozturk M**, **Tamgue O**, **Parihar SP**, **Kawaji H**, **Itoh M**, **Lassmann T**, **Carninci P**, **Hayashizaki Y**, **Forrest ARR**, **Guler R**, **Bajic VB**, **Brombacher F**, **Suzuki H.** Transcriptional landscape of *Mycobacterium tuberculosis* infection in macrophages. *Sci Rep* 8: 6758, 2018. doi:10.1038/s41598-018-24509-6.
24. **Shi M**, **Sun J**, **Lu S**, **Qin J**, **Xi L**, **Zhang J.** Transcriptional profiling of macrophages infected with *Fonsecaea monophora*. *Mycoses* 62: 374–383, 2019. doi:10.1111/myc.12894.
25. **Labow BI**, **Souba WW**, **Abcouwer SF.** Glutamine synthetase expression in muscle is regulated by transcriptional and posttranscriptional mechanisms. *Am J Physiol Endocrinol Physiol* 276: E1136–E1145, 1999. doi:10.1152/ajpendo.1999.276.6.E1136.
26. **Qing G**, **Li B**, **Vu A**, **Skuli N**, **Walton ZE**, **Liu X**, **Mayes PA**, **Wise DR**, **Thompson CB**, **Maris JM**, **Hogarty MD**, **Simon MC.** ATF4 regulates MYC-mediated neuroblastoma cell death upon glutamine deprivation. *Cancer Cell* 22: 631–644, 2012. doi:10.1016/j.ccr.2012.09.021.
27. **Menchini RJ**, **Chaudhry FA.** Multifaceted regulation of the system A transporter Slc38a2 suggests nanoscale regulation of amino acid metabolism and cellular signaling. *Neuropharmacology* 161: 107789, 2019. doi:10.1016/j.neuropharm.2019.107789.
28. **Chen R**, **Zheng S**, **Zhao X**, **Huang H**, **Xu Y**, **Qiu C**, **Li S**, **Liang X**, **Mao P**, **Yan Y**, **Lin Y**, **Song S**, **Cai W**, **Guan H**, **Yao Y**, **Zhu W**, **Shi X**, **Ganapathy V**, **Kou L.** Metabolic reprogramming of macrophages by a nano-sized opsonization strategy to restore M1/M2 balance for osteoarthritis therapy. *J Control Release* 380: 469–489, 2025. doi:10.1016/j.jconrel.2025.02.005.

Downloaded from journals.physiology.org/journal/ajpcell at Univ Degli Studi Di Parma Biblio Centrale (160.078.086.043) on September 21, 2026.

29. **Gauthier-Coles G**, **Vennitti J**, **Zhang Z**, **Comb WC**, **Xing S**, **Javed K**, **Broer A**, **Broer S.** Quantitative modelling of amino acid transport and homeostasis in mammalian cells. *Nat Commun* 12: 5282, 2021. doi:10.1038/s41467-021-25563-x.
30. **Baird FE**, **Beattie KJ**, **Hyde AR**, **Ganapathy V**, **Rennie MJ**, **Taylor PM.** Bidirectional substrate fluxes through the system N (SNAT5) glutamine transporter may determine net glutamine flux in rat liver. *J Physiol* 559: 367–381, 2004. doi:10.1113/jphysiol.2003.060293.
31. **Baird FE**, **Pinilla-Tenas JJ**, **Ogilvie WL**, **Ganapathy V**, **Hundal HS**, **Taylor PM.** Evidence for allosteric regulation of pH-sensitive System A (SNAT2) and System N (SNAT5) amino acid transporter activity involving a conserved histidine residue. *Biochem J* 397: 369–375, 2006. doi:10.1042/BJ20060026.
32. **Oppedisano F**, **Pochini L**, **Galluccio M**, **Indiveri C.** The glutamine/amino acid transporter (ASCT2) reconstituted in liposomes: transport mechanism, regulation by ATP and characterization of the glutamine/glutamate antiport. *Biochim Biophys Acta* 1768: 291–298, 2007. doi:10.1016/j.bbamem.2006.09.002.
33. **Tan Z**, **Xie N**, **Banerjee S**, **Cui H**, **Fu M**, **Thannickal VJ**, **Liu G.** The monocarboxylate transporter 4 is required for glycolytic reprogramming and inflammatory response in macrophages. *J Biol Chem* 290: 46–55, 2015. doi:10.1074/jbc.M114.603589.
34. **Knut & Alice Wallenberg Foundation.** The Human Protein Atlas (Online). https://www.proteinatlas.org/search/SLC38A5 [2025 Aug 9].
35. **Alasoo K**, **Martinez FO**, **Hale C**, **Gordon S**, **Powrie F**, **Dougan G**, **Mukhopadhyay S**, **Gaffney DJ.** Transcriptional profiling of macrophages derived from monocytes and iPS cells identifies a conserved response to LPS and novel alternative transcription. *Sci Rep* 5: 12524, 2015. doi:10.1038/srep12524.
36. **Cobo I**, **Cheng A**, **Murillo-Saich J**, **Coras R**, **Torres A**, **Abe Y**, **Lana AJ**, **Schlachetzki J**, **Liu-Bryan R**, **Terkeltaub R**, **Sanchez-Lopez E**, **Glass CK**, **Guma M.** Monosodium urate crystals regulate a unique JNK-dependent macrophage metabolic and inflammatory response. *Cell Rep* 38: 110489, 2022. doi:10.1016/j.celrep.2022.110489.
37. **Zielińska M**, **Dąbrowska K**, **Hadera MG**, **Sonnewald U**, **Albrecht J.** System N transporters are critical for glutamine release and modulate metabolic fluxes of glucose and acetate in cultured cortical astrocytes: changes induced by ammonia. *J Neurochem* 136: 329–338, 2016. doi:10.1111/jnc.13376.
38. **Taurino G**, **Deshmukh R**, **Villar VH**, **Chiu M**, **Shaw R**, **Hedley A**, **Shokry E**, **Sumpton D**, **Dander E**, **D'Amico G**, **Bussolati O**, **Tardito S.** Mesenchymal stromal cells cultured in physiological conditions sustain citrate secretion with glutamate anaplerosis. *Mol Metab* 63: 101532, 2022. doi:10.1016/j.molmet.2022.101532.
39. **Chiu M**, **Taurino G**, **Dander E**, **Bardelli D**, **Fallati A**, **Andreoli R**, **Bianchi MG**, **Carubbi C**, **Pozzi G**, **Galuppo L**, **Mirandola P**, **Rizzari C**, **Tardito S**, **Biondi A**, **D'Amico G**, **Bussolati O.** ALL blasts drive primary mesenchymal stromal cells to increase asparagine availability during asparaginase treatment. *Blood Adv* 5: 5164–5178, 2021. doi:10.1182/bloodadvances.2020004041.
40. **Taurino G**, **Griffini E**, **Toscani D**, **Maccari C**, **Tardito S**, **Bianchi MG**, **Casati L**, **Dander E**, **D'Amico G**, **Andreoli R**, **Giuliani N**, **Bussolati O**, **Chiu M.** A metabolic trade-off between malignant plasma cells and mesenchymal stromal cells sustains multiple myeloma growth. *Blood Neoplasia* 3: 100195, 2026. doi:10.1016/j.bneo.2026.100195.
41. **Liu Y**, **Guo J**, **Xu H**, **Xu X**, **Jin X**, **Zhang Y**, **Qiu Y.** Glutamine-mediated crosstalk between M2 macrophages and tumor cells via the SLC38A5/FOXM1/CNIH4 axis promotes oral squamous cell carcinoma progression. *J Transl Med* 24: 423, 2026. doi:10.1186/s12967-026-07875-y.
42. **Shang M**, **Cappellesso F**, **Amorim R**, **Serneels J**, **Virga F**, **Eelen G**, **Carobbio S**, **Rincon MY**, **Maechler P**, **De Bock K**, **Ho PC**, **Sandri M**, **Ghesquiere B**, **Carmeliet P**, **Di Matteo M**, **Berardi E**, **Mazzone M.** Macrophage-derived glutamine boosts satellite cells and muscle regeneration. *Nature* 587: 626–631, 2020. doi:10.1038/s41586-020-2857-9.
43. **Yang M**, **Chen X**, **Hu X**, **Li H**, **Huang H**, **Fang Y**, **Jiang J**, **Liu H**, **Wang Y**, **Qing G.** The NF-kappaB-SLC7A11 axis regulates ferroptosis sensitivity in inflammatory macrophages. *Cell Insight* 4: 100257, 2025. doi:10.1016/j.cellin.2025.100257.
44. **Zhu X**, **Chen Y**, **Xu B**, **Mou J**, **Wang M**, **Gu Q**, **Sun Q**, **Li M**, **Zhao C**, **Zeng M**, **Lv Y**, **Zhang S**, **Bai X**, **Du J**, **Yu H**, **Liu M**, **Luo X**, **Li J**, **Hu S**, **Jia H**, **Yu B.** Targeting KEAP1/NRF2 interaction with oleuropein ameliorates atherosclerosis by inhibiting macrophage ferroptosis. *Free Radic Biol Med* 240: 566–582, 2025. doi:10.1016/j.freeradbiomed.2025.08.036.

Downloaded from journals.physiology.org/journal/ajpcell at Univ Degli Studi Di Parma Biblio Centrale (160.078.086.043) on September 21, 2026.